Records of East Asian monsoon activities in Northeastern China since 15.6 ka, based on grain size analysis of peaty sediments in the Changbai Mountains

Nannan Li[a], Frank M. Chambers[b], Jinxiu Yang[a,c], Dongmei Jie[a,d,e*], Lidan Liu[a], Hongyan Liu[a], Guizai Gao[a], Zhuo Gao[a], Dehui Li[a], Jichen Shi[a], Yingying Feng[a], Zhihe Qiao[f]

a. School of Geographical Sciences, Northeast Normal University, Changchun 130024, China

b. Centre for Environmental Change and Quaternary Research, School of Natural and Social Sciences, University of Gloucestershire, Francis Close Hall, Swindon Rd, Cheltenham, GL50 4AZ, UK

c. Dafeng Middle school of Chengdu, Chengdu 610000, China

d. Key Laboratory for Wetland Ecology and vegetation Restoration, Ministry of Environmental Protection, Changchun 130024, China

e. Key Laboratory of Vegetation Ecology, Ministry of Education, Changchun 130024, China

f. Daqing Normal University, Daqing 163712, China

*Corresponding author: Dr. Dongmei Jie, Email:jiedongmei@nenu.edu.cn

Abstract: Peatlands provide a widespread terrestrial archive for Holocene study. However, little is known about the grain-size characteristics of peaty sediments and their environmental significance. In order to study these phenomena in detail, two sections from the Hani and Gushantun peatlands in the Changbai Mountain Area were cored and sub-sampled. Based on reliable calibrated AMS ^{14}C ages, we established grain size variations in the peat cores since 15.6 ka cal. BP. Our results showed that the peaty sediments in the Changbai Mountains are mainly composed of silt. Moreover, the grain size component, which is related to paleoclimate variables, can be classified into three groups based on the "Grain size class *vs.* standard deviation" method. These sensitive grain size components are <37.0 μm (Component 1 or C1), 37.0–497.8 μm (Component 2 or C2) and >497.8 μm (Component 3 or C3). C1 comprises the finest silt in the peaty sediment and is mainly conveyed by the East Asian winter monsoon (EAWM), whereas C2 is transported into the peatland by surface runoff related to the enhancement of the East Asian summer monsoon (EASM). C3 is conveyed in saltation and bed-load mode by strong surface runoff linked to high-energy flow caused by a strong EASM, and perhaps is an indicator of extreme rainfall events in the Changbai Mountains. Our results suggest that the study region was dominated by a cold/dry environment during the late-glacial period under a strong EAWM. However, there was a marked climatic shift from an EAWM-dominated cold/dry climate to an EASM-dominated more mesic environment during the early Holocene. Increased percentage of C2 in peat cores during the Holocene Optimum (9.0–4.5 ka) indicates abundant rainfall in the study region (even with extreme rainfall events) as a result of a significant enhancement of the EASM. Weak monsoon events occurred at 10.5 ka, 9.2 ka, 8.2 ka, 7.2 ka, 6.2ka, 5.5 ka and 4.2 ka shown by sharp decreases in C2, agreeing with the stalagmite δ^{18}O records in China. The results obtained from environmentally

sensitive grain-size component records are largely consistent with other palaeoenvironmental records in the East Asian monsoon area, substantiating the regional climate patterns and monsoon evolution since late-glacial time. Because intensity of the East Asian monsoon is likely responsible for the grain-size change in the peat samples, the grain size components in peat samples may be used for reconstructions of past environmental conditions and of variability in the East Asian monsoon.

Keywords: Peatland; Grain-size; East Asian monsoon; Holocene; Changbai Mountains

1. Introduction

Peatlands provide a widespread archive of Holocene environmental change. Because the sampling of peat is relatively simple, the range of paleoclimate evidence and proxies is wide, and dating methods have become more accurate, such that peatlands have great potential for Holocene research (Chambers and Charman, 2004) and particularly for palaeoclimate reconstruction (Chambers et al., 2012), exemplified variously by studies in Europe (Barber et al., 2003), North America (Klein et al., 2013), South America (Chambers et al., 2014) and Siberia (Smith et al., 2004). Increasingly, there has been use of peat archives in China (e.g. Makohonienko et al., 2004; Ma et al., 2009; Zhou et al., 2010; Zhao et al., 2011; Gao et al., 2014; Zhao et al., 2014). Indeed, Northeastern (NE) China is one of the most important peat distribution regions of the world (Chai, 1990). Up to now, several Holocene paleoclimate reconstructions have been carried out using peat deposits in the Changbai Mountains, and many proxies have been used as indicators to study Holocene environment change, including pollen (Liu et al., 1989; Xu et al., 1994; Xia and Wang, 2000; Makohonienko et al., 2004), phytolith (Zhang et al., 2007; Guo et al., 2012), stable isotopes (Hong et al., 2009, 2010), testate amoebae (Li et al., 2009), chemical element (Zhang et al., 2011) and biomarkers (Zhou et al., 2010). However, the inorganic mineral composition of peat deposits has been overlooked, yet grain size is recognized as an important paleoenvironmental proxy in other depositional environments (Liu, 1985; Ding et al., 1998; Lu and An, 1998; Sun et al., 2003; Huang et al., 2011; Qiao et al., 2011). There are relatively few published studies using the grain size of mineral clasts in peat as a paleoenvironmental indicator to reconstruct Holocene climate change (Wang et al., 2003; Yu et al., 2006; Bao et al., 2010; Zhang et al., 2014); indeed, there has been a lack of systematic study of the grain-size characteristics of peaty sediments and their environmental significance.

The Changbai Mountains are located at the northern periphery of the East Asian summer monsoon (EASM). Since the Last Glaciation, paleoclimate fluctuations and the swings of the monsoon boundary (Wang et al., 2001, 2005, 2008; Wang et al., 2005a; Stebich et al., 2015) must have changed the sedimentary environments of peatlands, and these changes may be reflected in the grain size characteristics of peat deposits. Thus, peatland may have great potential to investigate the activities history of the EAM. In this study, two cores of peat that accumulated since the late-glacial time were taken from the Changbai Mountains, NE China. Combined with high-precision AMS ^{14}C dating, we focused on grain size characteristics of mineral clasts within the peat deposit and its environmental significance. To facilitate more reliable reconstructions, grain-size class *vs.* standard deviation was used to obtain environmentally sensitive components of

the peat sediments. Based on the time sequences of these components, we present an inferred variation history of the EAM and paleoclimatic changes in the Changbai Mountains since the late-glacial time.

2. Regional setting

Hani (42°13'31.1" N, 126°30' 14.7" E, 890m a.s.l.) and Gushantun (42°18'22.1" N, 126°16' 57.7" E, 506m a.s.l.) peatlands are situated west of the Changbai Mountains (Fig. 1 A and B) in the Longgang Volcanic Field, which is an area of active vulcanicity in China (Liu, 1988). There were intense Cenozoic volcanic activities in this region and these provided a geological basis for the development of peatland. The lake basin substrate of the Hani peatland is Early Pleistocene basalts (Isotopic Age of 2.6 ± 0.29 Ma (Qiao, 1993)). In the Late Pleistocene, the Hani River valley was dammed during the Nanping Period by volcanic ejecta. Since then, peat formed in the former lake basin (Qiao, 1993). The Gushantun peatland is also surrounded by Cenozoic basalt, with the peatland initiated in the Late Pleistocene on a former Maar Lake (Zhao and Hall, 2015). The average thickness of the peat is about 7 m.

The modern climate of NE China is controlled by the EAM, which shows strong seasonal variability. Dominating north-westerly winds in winter contribute aeolian material from the interior of the Eurasian land mass to the Changbai Mountains (Schettler et al., 2006a, 2006b, 2006c). In contrast, summers are dominated by humid air, transported by south-easterly winds from the Pacific. So the regional precipitation period is concentrated from June to August (Fig.1 C). The average annual temperature of Changbai Mountains ranges from -7.3 °C to 4.8 °C while the average annual rainfall ranges from 700 mm to 1400 mm (Wang, 1989). The landform type in the Changbai Mountains is diverse, with catenae of mountain, plateau, tableland and valley (Fig.1 B). The dominant soil in the study region is dark brown forest soil, but with meadow soils in valleys and lessive soil on high tableland. Moreover, the Changbai Mountains are situated in the modern temperate conifer–hardwood forest zone, representing one of the best preserved primeval forests in China.

3. Material and methods

3.1 Sampling and chronology

Peat sediment cores were taken from the Hani and Gushantun peatlands (Fig. 1) in the summer of 2009, using an Eijkelkamp peat sampler. The length of the Hani (HN) core was 350 cm while that from Gushantun (GST) was 750 cm. Both cores were sub-sampled at 1-cm intervals, resulting in 350 sub-samples from Hani and 750 from Gushantun. Reflecting changes in lithology, sixteen bulk organic samples were dated by accelerator mass spectrometry (AMS) radiocarbon dating at Peking University. All the radiocarbon ages were calibrated into calendar ages before present (BP) (Table 1) with the Intcal13 calibration data (Reimer et al., 2013) using the CALIB Rev. 7.0.4 program (Stuiver and Reimer, 1993) and chronologies were estimated with the Bacon v2.2 model (Fig. 2) (Blaauw and Christen, 2011). Meanwhile, in order to investigate the environmental significance of different components in peat, three dust samples were collected using a glass dust collection tank (15 cm in diameter and 30 cm in depth) from Nov., 2010 to May, 2011. The tank is located at Hani Automatic Weather Station and about 3m off the ground.

3.2 Grain size analysis

Peat samples were selected at 2-cm intervals for the Hani section and 10-cm intervals from the Gushantun section for grain size analyses. Before any further treatment, all samples were dried in a thermostatic drying chamber at 105 °C.

In advance of grain size measurements, *c*. 0.5 g dry peat samples were pretreated in a muffle furnace (550 °C) for 4 hours to remove organic matter (Lewis, 1989), while dustfall samples were pretreated using 30% hydrogen peroxide (H_2O_2). Then, all samples were treated with 10% hydrochloric acid (HCl) to remove carbonates and with 10 mL 0.05 mol/L sodium hexametaphosphate ($(NaPO_3)_6$) to facilitate dispersion. The grain size distribution was determined with a MICROTRAC S3500 particle analyzer at Northeast Normal University. It automatically yields the percentages of the clay-, silt- and sand-size fractions and the median diameter over the range of 0.02–2800 μm. Replicate analyses indicated that the mean grain size has an analytical error of 2%.

3.3 Mathematical method

The grain-size characteristics of sediments are sensitive to a change in transport process (Visher, 1969). The grain-size distribution of clastic deposits with a single provenance should show a unimodal, symmetric distribution (Friedman and Sanders, 1978; Ashley, 1978). However, when the shape of a grain-size distribution is asymmetric or skewed, the sediment is considered to be combined from multiple sources (Friedman and Sanders, 1978; Ashley, 1978; Xiao et al., 2012). As the sedimentary processes of modern or geologic deposits are usually influenced by multiple transport dynamics, the grain-size distribution shape is usually asymmetric and skewed (Visher, 1969; Friedman and Sanders, 1978; Ashley, 1978).

Thus, if using parameters that describe the grain size distribution of a total sample (i.e. Mz), it may lead to the loss of some information that appears minor but is important in a sample. Increasingly over recent years, mathematical methods have been used to extract the grain size components from a total sediment (Sun et al., 2001; Boulay et al., 2003; Sun et al., 2003; Xiao et al.,2012; Zhang et al., 2014). Among them, "Grain size class *vs.* standard deviation" is easy to calculate. It was first proposed by Boulay and applied to marine paleoenvironment reconstruction (Boulay et al., 2003). Now it has been widely used in many Quaternary paleoclimate fields (e.g. Fan, et al., 2011; Xu and Wang, 2011; Guan et al., 2013; Zhou et al., 2014). In this study, we selected this method to obtain environmentally sensitive components of the peat sediments.

4. Results

4.1 Grain size characteristics of peat and modern dustfalls

According to the Wentworth (1922) and Link (1966) sediment classification system, peaty sediments from the two profiles resemble each other in texture and grain size distribution. The peat sediment is dominated by silt, whose percentage is more than 50% (Fig. 3), with the grain size frequency distribution concentrated in the range 1 to 350 μm (Fig. 4.a, 4.b). Grain size frequency distributions of the peat deposits show unimodal (Fig. 4.a) and multimodal (Fig. 4.b) distributions, indicating the change of sediment sources and transport dynamics.

The grain size distribution of dustfall samples is mainly within the range 1 to 100 μm and the

mean size varies from 12 to 17 μm (Fig. 4.c). Moreover, the grain size frequency of dustfall samples shows regular unimodal distributions, which indicates the typical well-sorted character of aeolian deposits (Pye, 1987). By comparing the grain size distribution of peat and dustfall samples, it can be shown that aeolian deposits only contribute to the fine-grain components in a peat sample. Coarser particles must be transported by other processes into the peatland, such as by surface runoff. It is therefore likely to be misleading merely to use the general grain size parameters in paleoenvironment reconstruction, and it is preferable to extract different sedimentary components from a total sample using mathematical methods.

4.2 Extraction of environmentally sensitive components

Grain-size class *vs.* standard deviation values of the peat samples are shown in Table 2 and displayed in Fig. 5 (which also shows the grain size distribution of the dustfall, for comparison). Although the standard deviation values of Hani peat are smaller than those of Gushantun (except for the >500.0 μm part), the shape of the curves and the number of the sensitive grain size components for the two cores show good agreement (Fig. 5). Taking section Gushantun as an example, there are three distinct peaks on the grain size class standard deviation curves, corresponding to 13.0 μm, 209.3 μm and 837.2 μm, whereas the grain size values of troughs are 37.0 μm and 592.0 μm (Fig. 5). Taking the two curves together, two troughs (37.0 μm and 497.8 μm) divide each curve into three components in each peat core: <37.0 μm (Component 1 or C1), 37.0–497.8 μm (Component 2 or C2) and >497.8 μm (Component 3 or C3).

5. Discussion

5.1 Implication of each sensitive grain size component in peat cores

Results of grain size class *vs.* standard deviation show that there are three components in peat sediments (Fig.5). As different grain size components resulted from different transport processes, each component has different environmental implications in the East Asian monsoon area (EAMA).

Of the three components, the <37.0 μm particles (Component 1) comprise the finest silt (Wentworth, 1922) in peat. The grain size of this component shows a good correlation with the particle size of modern dustfalls collected in Hani peatland whose <37.0 μm particles account for more than 90% of the clastic deposition (Fig. 5). This suggests that C1 was transported in suspension mode by the wind (Patterson and Gillette, 1977; Pye, 1987).

During the winter and spring, NE China was frequently influenced by duststorms under the control of strong Mongolia–Siberian high atmospheric pressure (Zhang et al., 2005; Jie et al., 2010). Sandy lands are widely distributed in the semi-humid and semi-arid region of NE China (e.g. Songnen Sandy Land, Horqin Sandy Land and Hulunbeier Sandy Land), and their eastern boundary is *c*. 200 km from the study region. These sandy lands are important clastic sources for duststorms in NE China. In addition, because relief in NE China is high in the east but lower in the west, it can be envisaged that strong northwesterly winds in winter would convey C1 (<37.0 μm population) towards the eastern part of NE China and deposit in peatland when encountering the high Changbai Mountains (process (1) in Fig. 6). Especially during episodes of cold and dry climate, fixed dunes were activated and the sandy lands expanded in the west part of NE China (Qiu, 1989; Li, 1991). Hence, the winter monsoon blows fine silt from the west sandy lands and

eventually deposits it in peatlands in the Changbai Mountains (process (1) in Fig. 6).

Over recent years, several studies have confirmed the contribution of aeolian dust to the sediments in the Changbai Mountains. For example, by investigating clay mineralogical characteristics and pedogenic processes of volcanic ash soils in the Changbai Mountains, Zhao et al. (1997) inferred that pedogenic processes were strongly associated with the influence of tropospheric aeolian dust from arid and semi-arid regions in China and Mongolia under cold or dry environments. Bao et al. (2009, 2010) also proposed that part of peat mineral material was transported to peatland by long-range aeolian dust and short-distance dust. Geochemical evidence from Lake Sihailongwan (*c*. 12 km from Hani peatlands) showed that the siliciclastic fraction of Holocene sediments is largely represented by aeolian influx of clay- to silt-sized debris of remote provenance (Schettler et al., 2006b, 2006c). These previous studies imply that aeolian dusts from North China areas contribute to the fine-grain clasts of the peat sediments. Thus, in this study, we hypothesize that C1 is mainly transported by winds and has a high sensitivity to the East Asian winter monsoon (EAWM); it can be considered as a proxy of the EAWM. The greater the content of C1 in the peat section, the stronger was the EAWM episode.

Component 2 (37.0–497.8 μm grain-size population) mainly consists of coarse silt and sand. As the dustfalls in peatland only contribute fine silt particles to peat clastics, the coarse clastic grains (C2) in peat samples must be transported into the peatland by other processes. Surface runoff in the valley is most likely responsible for this. Because high rainfall intensity would enhance soil erosion over the mountain area and increase the transport capacity of streams and runoff, coarse clasts would be available for runoff transportation and subsequent deposition in a peatland (process (2) in Fig. 6) (Hakanson and Jansson, 1983; Li et al., 2014). In the EAMA, regional rainfall is concentrated in summer. Thus, the more rainfall in the study region, the stronger is the runoff into the valley, which would lead to a higher C2 content in peat deposits. As the intensity and frequency of rainfall in NE China are controlled by the East Asian summer monsoon (EASM), so C2 can be regarded as its proxy.

Component 3 (>497.8 μm population) is the coarsest component in peat samples. It is conveyed in saltation and bed-load mode by strong flow currents (Visher, 1969; Ashley, 1978; Friedman and Sanders, 1978; Lewis, 1989). Only under severe rainfall can it be transported into the peatland. In the EAMA, if the strength of the EASM enhanced significantly, surface runoff originating from heavy rainfall can bring C3 into the peatland (like process (2) in Fig. 6). Thus, C3 is closely linked to strong runoff caused by the strong EASM and it can be used to reconstruct extreme rainfall events in the Changbai Mountains.

5.2 Paleoenvironmental reconstruction

Studies of speleothems in China have shown that shifts in the stable oxygen isotope ratio ($\delta^{18}O$) of cave stalagmite largely reflect changes in $\delta^{18}O$ values of meteoric precipitation in the EAMA, which in turn relate to changes in the amount of precipitation and thus characterize the Asian monsoon strength (e.g. Wang et al., 2001; Wang et al., 2005; Dykoski et al., 2005). According to several stalagmite $\delta^{18}O$ records (i.e. Hulu Cave (Wang et al., 2001); Dongge Cave (Wang et al., 2005; Dykoski et al., 2005); Shanbao Cave (Shao et al., 2006)), the history of EASM activities since the late-glacial time in China has been well established. Moreover, multi-proxy studies of the Hani peatland (i.e. pollen (Cui et al., 2006; Yu et al., 2008); $\delta^{18}O$ (Hong et al., 2009) and $\delta^{13}C$ (Hong et al., 2010) of cellulose, etc.) have been used for paleoenvironmental and paleoclimate

reconstruction. Those reconstructions provide comparators for assessing how well the grain sizes of peaty sediments can reflect the activities of the East Asian monsoon.

According to Fig. 7 and Fig. 8, variations of different components (C1, C2) in the two peat cores are in-phase. This suggests that mineral particle deposition in peatlands was forced by the same factor (or factors), which most likely were related to regional climate rather than to site-specific changes. As different components share different environmental implications, the variation of each component can be used to reconstruct paleoenvironmental evolution in NE China.

5.2.1 Cold and dry climate in late-glacial period

During the late-glacial period (15.6 ka cal. BP to 11.6 ka cal. BP in this study), C1 was high in both peat sections (Fig. 7). Its content was generally stable at more than 60%, while the percentages of C2 were not higher than 30%, indicating that NE China was dominated by the EAWM as clastic sediments were mainly transported into the peatland by wind. This is mainly consistent with other proxy reconstruction results in NE China. For example, pollen data from the Hani peatland show that the late-glacial period is characterized by herb pollen proportions of roughly 40–60%. *Artemisia* values represent around 40%, indicating a dry and cold climate (Yu et al., 2008). Similarly, pollen data from marr lakes (Liu et al., 2008; Stebich et al., 2009) and other peatland cores (Liu et al., 1989) have shown the same dry/cold late-glacial paleoclimate pattern in NE China. It is mostly because the semi-arid climate and strong EAWM during the late-glacial period were conducive to aeolian transport that more C1 was taken into the peatland. Optical stimulated luminescence (OSL) dating shows that the basal ages of sections from Horqin Sandy Land were concentrated in the late-glacial period (Zhao et al., 2005; Yang and Yue, 2013), suggesting the sandy lands were activated and expanded under cold/dry environments and higher wind strengths. Under the control of a strong EAWM, northwesterly winds blew strongly over the surface of the sandy land, resulting in removal of fine-grained material and retention of coarse grains. Yi et al. (2013) found that percentages of >63 μm components from many profiles in the Horqin Sandy Land increased dramatically during the late-glacial period, corresponding to the removal of fine grains under strong winds. The result is a significant increase of dust accumulation in the Changbai Mountains peat cores.

Overall, the regional late-glacial paleoclimate in the study area can be characterized as cold and dry, but there was still a series of climate fluctuations. During 14.5 to 13.2 ka, a slight increase of C2 indicates a temporary enhancement of the EASM (Fig. 8.a). This corresponds with the lighter shift of $\delta^{18}O$ in Dongge Cave, which seemingly correlates with the Bølling–Allerød warm period in Greenland (Johnsen et al., 2001). This interlude of favorable climate is also recorded by increases in thermophilous taxa pollen (Stebich et al., 2009), total organic carbon (TOC) and total nitrogen (TN) in sediments from Lake Sihailongwan (Schettler et al., 2006a; Parplies et al., 2008). At *c*. 13 ka cal. BP, the C2 content began to decrease in both peat cores, which corresponded to the beginning of the Younger Dryas (YD) as recorded in Greenland (Johnsen et al., 2001). However, the content of C2 showed a slight increase in the peat cores during 12.3 to 11.8 ka, indicating a temporary enhancement of the EASM. At the end of the YD, the content of C2 decreased again, showing a weakened summer monsoon. The abrupt enhancement of the EASM in the middle stage of the YD may correspond to the negative shift of peat cellulose $\delta^{13}C$ in Hani peatland, which has been attributed to a temporary strengthening of the EASM and a concurrent increase in

precipitation (Hong et al., 2010). It can be inferred that the regional climate experienced a complex "dry–wet–dry" cycle, as revealed by the grain size components in peaty samples during the YD (Fig. 8).

5.2.2 Instability of Holocene climate

At *c*. 11.3 ka, percentages of C2 from the Hani and Gushantun peat cores began to increase (Fig. 8) while C1 started to decline (Fig. 7), indicating a change in regional climatic pattern. Compared with the cold/dry climate in the late-glacial period, the EASM was significantly enhanced and rainfall increased concurrently in the early Holocene. As a result, more C2 was taken into the peatland by surface runoff. In the EAMA, stalagmite $\delta^{18}O$ values start to get lighter gradually during the early Holocene (Fig.8) (Dykoski et al., 2005; Shao et al., 2006; Wu et al., 2011). Pollen analyses show a gradual increase of temperate broadleaf pollen taxa and Cyperaceae pollen in the Hani peatland (Fig.7.A). A similar change was also recorded at Lake Erlongwan and Sihailongwan, where there was a transformation from the late-glacial coniferous-dominated vegetation to the Holocene coniferous–broadleaved forest (Liu et al., 2009; Stebich et al., 2015). However, in the Hani section there is an abrupt decrease of C2 at 10.7 ka to less than 30% that then lasted for 1500 years. Huang et al. (2015) discovered a 25 cm thick tephra layer at a depth of 600~625 cm in Hani peatland. Using AMS ^{14}C dating and age-depth modeling, they deduced this tephra layer deposited from 10.7~9.3 ka cal. BP. In our study, the decrease of C2 approximately corresponds to the time span of the tephra layer. So we suggest that the tephra layer, which formed during 10.7~9.3 ka, affected the measurement of grain size. However, unlike Hani peatland, there is presently no report of this tephra layer discovered in the Gushantun peatland. So this may be the reason for the discrepancy between Hani and Gushantun records during the early Holocene.

In the western part of NE China, the early Holocene was characterized by low sand content and higher magnetic susceptibility in the Horqin Sandy Land (Yi et al., 2013). The first paleosol layer developed during 10.0 to 7.0 ka cal. BP, indicating a relatively moist climate (Qiu et al., 1992). As a result, the wind-blown activity weakened and then mobile sand dunes were fixed as the land areas became blanketed with vegetation (Qiu et al., 1992). Hence, the fine grains (C1) transported by the EAWM reduced in peat cores in the Changbai Mountains. All the previous results suggest the climate pattern in NE China changed significantly during the early Holocene. Our reconstruction results based on environmentally sensitive grain-size components are in agreement with other proxy records in the EAMA.

The mid-Holocene is characterized by a warm and moist climate, reflected by higher percentages of C2 from 9.0 to 4.5 ka cal. BP (Fig. 8). C2 values increased gradually in the early Holocene and reached the largest percentages in the mid-Holocene, while C1 showed a marked decline (Fig. 7). This indicates that, under the control of a strong EASM, surface runoff caused by regional rainfall transported more coarse clastics into the peatland. This is almost synchronous with the negative shift of stalagmite $\delta^{18}O$ records (Fig.8) in Dongge Cave (Dykoski et al., 2005), Shanbao Cave (Shao et al., 2006) and Nuanhe Cave (Wu et al., 2011). Paleoenvironmental reconstruction from Hani peatland showed that there was a considerable expansion of broadleaf deciduous trees from 9.3 ka to 4.5 ka (Yu et al., 2008) and the variation in total broadleaf pollen percentages is almost synchronous with that of C2 (Fig.7). The percentages of broadleaf pollen such as *Juglans* and *Ulmus* reached their peaks (above 10%) in the section, while Cyperaceae reached their maximum (above 20%) (Fig.7), indicating a more warm and humid climate around

the Hani peatland (Yu et al., 2008). In the Changbai Mountains, Liu et al. (2009) proposed that Lake Erlongwan was surrounded by dense *Quercus–Ulmus–Juglans* dominated temperate broadleaf deciduous forests during the "Holocene Optimum" (HO). Stebich et al. (2015) also suggested a development of broadleaf trees (*Juglans*, *Quercus* and *Ulmus*) during the mid-Holocene. According to pollen analysis of peat cores in the Changbai Mountains, Yuan and Sun (1990) proposed boreal conifers virtually disappear from the study region during 9.0 to 4.0 ka as indicated by only scattered occurrences of conifer pollen (*Picea*, *Abies*, *Larix*). Owing to the high temperature and humidity, most of the peat decomposed and a sapropel layer formed (Yuan and Sun, 1990).

The end of the "Holocene Optimum" warm phase is suggested by a sharp decrease of C2 content at ~4.2 ka. This is contemporaneous with the abrupt positive shift of stalagmite $\delta^{18}O$ records in Shanbao Cave (Shao et al., 2006). C2 content dropped almost to values of the late-glacial time (Fig. 8) while C1 sharply increased (Fig. 7) during *c*. 3.8 to 1.8 ka cal. BP, indicating the Holocene Optimum was interrupted by a weak monsoon episode. In the Changbai Mountains, pollen analysis showed that the Hani peatland was surrounded by conifer-dominated forest during 3.8 to 1.4 ka cal. BP (Cui et al., 2006). Along with the declining values for pollen of broadleaf and hydrophilous plants, the study region experienced a cool/dry climate (Cui et al., 2006). Moreover, there was an interruption of stalagmite formation in Nuanhe Cave from 3.5 to 2.0 ka cal. BP (Fig. 8), denoting the cold and dry climate in NE China temporarily halted the Karst process (Wu et al., 2011). From 3.8 ka to 1.7 ka BP, sediments of the Horqin Sand Land became coarser and the dry/cold climate resuscitated the aeolian activities (Zhao et al., 2013). The peat section ML, located in the southeastern margin of the Horqin Sand Land, experienced a decrease of tree pollen and an increase of *Artemisia* and Chenopodiaceae pollen during the same period, suggesting a shift to a cool and dry climate (Ren and Zhang, 1997).

In the Late Holocene, there was a temporary enhancement of the EASM from 1.5 to 0.9 ka cal. BP, reflected by a marked increase of C2 (Fig. 8). The relatively favorable climate was recorded in LHT sand–paleosol sequence (1.7 to 1.0 ka) in the Horqin Sand Land (Zhao et al., 2013). Based on radiocarbon ages, Qiu et al. (1992) proposed that the last paleosol layer in Songnen Sandy Land developed during this period. In addition, results from pollen analysis also provided convincing evidence for the climate shift to a warm and wet period. Yang et al. (2001) proposed that there was a pollen concentration peak after 1.5 ka BP (1.43 ka cal. BP). At the same time, concentration of pollen in section ML sharply increased during 1.0 to 0.6 ka cal. BP; some pollen taxa even reached the largest value of the section (Ren and Zhang, 1997). Another peat core from NE China also showed a decrease of cryophilic plants pollen from 1.5 to 1.1 ka cal. BP (Zhang et al., 2004). All of these records show that NE China experienced a warm and wet regional environment in this phase.

The temporary favorable climate corresponds approximately to the Sui and Tang dynasties of China, and to the "medieval warm period (MWP)" in Europe (Lamb, 1965). Under the Sui and Tang dynasties, China enjoyed a period of prosperous population and economic expansion and perhaps it was inextricably linked to a favorable climate (Zhu, 1973). A cool and dry climate (equivalent to the Little Ice Age of Lamb (1980)) closely followed the MWP. Regional climate in NE China has fluctuated since the 19th century, but owing to conjectured human influence it may be difficult to identify subsequent natural climate changes.

Overall, indications of the EAM from the two peat cores, as reflected by the variation of

different grain size components, are similar. However, there are some inconsistencies in the paleoclimate patterns indicated by the two cores, especially during the middle to late Holocene (Fig.7 and Fig.8). As the distance between the two peatlands is *c*. 22 km, they are situated in the same climate and vegetation zone and even the geological substrates of the peatlands are similar. In theory, if the grain size character of clasts in peat is a reliable proxy to investigate the paleo-monsoon evolution, the two records should show very good agreement. Thus, any discrepancy between the two records must lie in the site-specific conditions of each peatland.

Hani peatland is located in the upper reaches of the Hani River with the river meandering through the center, while the Gushantun peatland does not have such a feature (Fig.1). The Hani River ranges 2~4 m in width and 0.5~1 m in depth (Qiao, 1993). Although the Hani peat section was not cored near the river, the variations of water flow and fluctuations of water level may have affected the sedimentary environment of the peatland.

As runoff controls the development of a river system, precipitation, which is closely linked to the runoff, plays an important role during the development of a river. In a monsoon region, more rainfall will contribute more surface runoff to shape the fluvial landforms. However, the fluvial action will be weakened under a dry/cold climate (Wang et al., 2009). As pointed out earlier, Hani peatland originated from an open valley dammed by volcanic ejecta during the Late Pleistocene. The course of the modern Hani River, which is now meandering in the peatland, developed later than (or simultaneously with) the initiation of the peatland. During the Last Glaciation, regional climate around the peatland was cold and dry, so the water flow of Hani River was low. However, the water flow started to increase as a result of the significant increase in precipitation during the Holocene Optimum (HO). Stronger water flow made the river larger, with a wide channel, resulting in further development of river landforms during the middle Holocene. Since then, the Hani River has made a far-reaching influence on the sedimentary environment of the peatland and it is possible this may be recorded in the peat section and be reflected in variation of percentages of different grain size components. Thus, the variation of C1 and C2 contents in the Hani peatland was influenced by both the activity of EAM and the Hani River flow capacity, which was related to both precipitation and groundwater supply.

In contrast with the Hani peatland, Gushantun peatland is free from the influence of a river and so the source of mineral clasts in peat is relatively simple. Fine grains conveyed by the wind and coarse grains transported by surface runoff resulted from the enhancement of rainfall, making contributions to the mineral clasts in the peatland. The percentages of the different components vary with fluctuations in the strength of the EAWM and EASM. This may be the reason why C1 and C2 of Gushantun Peat showed better correlation with other EAM proxies than that of Hani Peat (Fig.7 and Fig.8). Hence, when the influence of Hani River was not significant, such as during the late-glacial period and up to the mid-Holocene, variations of the C1 and C2 contents behaved similarly in both peatlands. The great development of the Hani River during the mid-Holocene is the main reason for the difference in the Hani record over the mid- to late Holocene.

Overall, as the paleoclimate evolution recorded by the different grain size components, especially the activity history of the East Asian monsoon, is broadly consistent with other proxy results for a large area of China, we contend that the grain size characteristics of clasts in peat are a reliable EAM proxy, both from theoretical analysis and empirical demonstration, as shown by this study. The technique can be used to investigate variation in history of the EAM in areas where

stalagmites are not easily accessible or are absent, but peatlands are widely distributed, such as in NE China. So it appears feasible to reconstruct the East Asian monsoon evolution using the grain size of mineral material in peat sediments. However, it also should be noted that while grain size of clasts in peat can be used as a proxy to investigate EAM evolution history, an enclosed peatland is preferable.

5.2.3 Global responses and paleo-climate events

During the Holocene, the EASM-dominated climate pattern was interrupted by several excursions, reflected by C2 content in each peat section (Fig. 8). The first EASM-weakened event occurred at 10.5 ka cal. BP and it correlated with a precipitation shift inferred from stalagmite $\delta^{18}O$ records in Dongge Cave (Dykoski et al., 2005) and Sanbao Cave (Shao et al., 2006), China. In particular, the percentages of C2 in the Gushantun peat core shift to smaller values by 40% at 10.5 ka (Fig. 8), reflecting an abrupt decrease in monsoonal rainfall. The second event occurred close to the 9.2 ka event observed in the ice cores from Greenland (Johnsen et al., 2001) and stalagmite $\delta^{18}O$ records in China (Dykoski et al., 2005; Shao et al., 2006). Around 9.2 ka in the Gushantun peat core (*c*. 9.6 ka in Hani section), percentages of C2 declined markedly while C1 increased (Fig. 7), indicating an enhancement of the EAWM and decrease in regional precipitation. The largest EASM-weakened event of the Holocene occurred at 8.2 ka, when the C2 content showed a dramatic shift by almost 50% (Fig. 8), apparently corresponding to the 8.2 ka BP event observed in Greenland (Johnsen et al., 2001). Following the likely 8.2 ka event, several abrupt shifts of C2 percentages in the two peat cores occurred at 7.2 ka, 6.2 ka, 5.5 ka and 4.2 ka (as shown in Fig.8). Most of these climate events have been reported from stalagmite $\delta^{18}O$ records in previous studies of the EAM (Wang et al., 2005). The consistent results between the environmentally sensitive grain size of peat sediments and high-resolution stalagmite $\delta^{18}O$ records as well as other records in the monsoon area demonstrate that it is feasible to use the grain size components to investigate the evolution of the EAM.

There is a series of extreme rainfall events recorded by peaty sediments in the Changbai Mountains. In NE China, a strong Asian summer monsoon event might induce an increase in both precipitation and potential high surface-water flow. As Component 3 (>497.8 μm population), the coarsest component in peat samples, was conveyed in saltation and bed-load mode by strong surface runoff under severe rainfall, the occurrence of C3 can be used for extreme rainfall events reconstruction (Fig.9). In order to test our reconstruction results, here we made a comparison between previous paleo-flood records (which were related to high-intensity rainfalls) at archaeological sites in the Yangtze River basin and the Yellow River basin (Yuan et al., 2002; Zhu et al., 1997; Wu et al., 2015; Zhang et al., 2002) and our reconstructed extreme rainfall events. It can be seen in Fig. 9 that our reconstruction was consistent with the other records. It appears that extreme rainfall events in the Changbai Mountains were concentrated in the Holocene Optimum. Perhaps, it indicates that cyclical extreme rainfall events in the Changbai Mountains during the mid-Holocene were related to the strength of the EASM.

6. Conclusion

In this paper we presented a detailed grain size analysis of two peat cores, dated by AMS ^{14}C, covering the Holocene from the Changbai Mountains, NE China. Conventional grain size parameters were complemented by the contents of extracted components with different origins

using the “Grain size class *vs.* standard deviation” method. Accordingly, a new late-glacial paleoclimate variation of the studied region has been established. In addition, long-term variations of the content of each component revealed the evolution of the East Asian monsoon, and reconstruction results were consistent with other regional and extra-regional records. The most important conclusions are summarized below.

(1) Peat sediments in the west foothills of the Changbai Mountains are mainly composed of silt. The grain size frequency distributions of the peat deposits showed unimodal and multimodal distributions, reflecting the differences in sediment sources and transport processes.

(2) Three sensitive grain size components were obtained: <37.0 μm (Component 1 or C1), 37.0–497.8 μm (Component 2 or C2) and >497.80 μm (Component 3 or C3). As C1 was mainly transported by winds and showed a high sensitivity to the EAWM, it can be considered as a proxy of the EAWM in the study region. A higher content of C1 usually resulted from a cold/dry climate. C2 in peat samples was transported into the peatland by surface runoff as a result of an increase in regional rainfall and can be regarded as a proxy of the EASM. Only under a significant enhancement of the EASM can C3 (the coarsest components in a peat sample) be transported into the peatland. Thus different components shared different environmental implications in the EAMA.

(3) During the late-glacial period, the study region was dominated by a strong EAWM, indicating NE China experienced cold and dry environmental conditions. Since the start of the Holocene, the data from peat cores in the Changbai Mountains showed a marked enhancement of the EASM, suggesting a climatic shift from EAWM-dominated cold/dry climate to an EASM-dominated favorable environment. The Holocene Optimum (9.0–4.5 ka) in NE China was characterized by abundant precipitation. Multiple weak Asian summer monsoon Events (10.5 ka, 9.2 ka, 8.2 ka, 7.2 ka, 6.2 ka, 5.5 ka and 4.2 ka) were recorded in the peat cores from Changbai Mountains. Moreover, extreme rainfall events occurred frequently during the Holocene Optimum in NE China and are synchronous between the two peat cores.

(4) Given the high degree of temporal coherence with previous reconstructed paleoclimate records from East Asia, it indicates that grain size of clasts in peaty sediments is also a convincing paleoclimatic proxy. It can be used to investigate the variation history of the East Asian monsoon for areas where stalagmites are not easily accessible or are absent, but peatlands are widely distributed, such as in NE China. Moreover, in contrast with other proxies used in the field of peatland study (e.g. pollen, $\delta^{13}C$), the pretreatment of grain size analysis is both straightforward and time-saving. However, it also should be noted that while grain size of clasts in peat was used as a proxy to investigate EAM evolution history, an enclosed peatland is preferable.

Acknowledgments

We thank Dr. Jinze Ma and Prof. Zhaojun Bu from Northeast Normal University for providing the dustfall samples collected in Hani peatland. This work was financially supported by the National Science Foundation of China (Grant No. 41471164, 40971116), the National Key Research and Development Project of China (Grant No. 2016YFA0602301) and the Foundation for Public Welfare Project funded by the Ministry of Environmental Protection of China (Grant No. 201109067). We thank Prof. Qingzhen Hao (CAS, Beiging) and Prof. Youbin Sun (CAS, Xi’an) for constructive discussion. We are grateful to Executive Guest Editor Hong-Chun Li and two

anonymous reviewers for their helpful reviews and suggestions.

References

Ashley, G.M., 1978. Interpretation of Polymodal Sediments. Journal of Geology 86(4), 411–421.

Bao, K., Jia, L., Wang, G., 2009. Characteristic and environmental significance of magnetic susceptibility of peat bog sediments in Changbai Mountains. Wetland Science 7(4), 321–326. (in Chinese).

Bao, K., Jia, L., Lu, X., Wang, G., 2010. Grain-size Characteristics of Sediment in Daniugou Peatland in Changbai Mountains, Northeast China: Implications for Atmospheric Dust Deposition. Chinese Geographical Science 20(6), 498–505.

Barber K.E., Chambers, F.M., Maddy, D., 2003. Holocene palaeoclimates from peat stratigraphy: macrofossil proxy climate records from three oceanic raised bogs in England and Ireland. Quaternary Science Reviews 22, 521–539.

Blaauw, M., Christen, J.A., 2011. Flexible paleoclimate age-depth models using an autoregressive gamma process. Bayesian Analysis 6, 457-474

Boulay, S., Colin, C., Trentesaux, A., Pluquet, F., Bertaux, J., Blamart, D., Buehring, C., Wang, P., 2003. Mineralogy and sedimentology of Pleistocene sediment in the South China Sea (ODP Site 1144). Proceedings of the Ocean Drilling Program Scientific Results 184, 1–21.

Chai, X., 1990. Peatland. Geological Publishing House, Beijing.

Chambers, F.M., Charman, D.J., 2004. Holocene environmental change: contributions from the peatland archive. The Holocene 14(1), 1–6.

Chambers, F.M., Booth, R.K., De Vleeschouwer, F., Lamentowicz, M., Le Roux, G., Mauquoy, D., Nichols, J.E., van Geel, B. 2012. Development and refinement of proxy-climate indicators from peats. Quaternary International 268, 21–33.

Chambers, F.M., Brain, S.A., Mauquoy, D.M., McCarroll, J., Daley, T., 2014. The Little Ice Age in the Southern Hemisphere in the context of the last 3000 years: peat-based proxy-climate data from Tierra del Fuego. The Holocene 24, 1649–1656.

Cui, M., Luo, Y., Sun, X., 2006. Paleoenvironmental and paleoclimate changes in Hani Lake, Jilin since 5ka BP. Marine Geology & Quaternary Geology 26(5), 117–122. (in Chinese).

Ding, Z., Sun, J., Liu, T., Zhu, R., Yang, S., Guo, B., 1998. Wind-blown origin of the Pliocene red clay formation in the central Loess Plateau, China. Earth and Planetary Science Letters 161, 135–143.

Dykoski, C.A., Edwards, R.L., Cheng, H., Yuan, D., Cai, Y., Zhang, M., Lin, Y., Qing, J., An, Z., Revenaugh, J., 2005. A high-resolution, absolute-dated Holocene and deglacial Asian monsoon record from Dongge Cave, China. Earth and Planetary Science Letters 233, 71–86.

Fan, D., Qi, H., Sun, X., Liu, Y., Yang, Z., 2011. Annual lamination and its sedimentary implications in the Yangtze River delta inferred from High-resolution biogenic silica and sensitive grain-size records. Continental Shelf Research 31, 129–137.

Friedman, G.M., Sanders J.E., 1978. Principles of sedimentology. Wiley, New York.

Gao, C., Lin, Q., Zhang, S., He, J., Lu, X., Wang, G., 2014. Historical trends of atmospheric black carbon on Sanjiang Plain as reconstructed from a 150-year peat record. Scientific Reports 4, 5723–5723.

Gao, Y., 1962. On some problems of Asian monsoon. In: Gao, Y. (Ed.), Some Questions about the

East Asian Monsoon. Chinese Science Press, Beijing. (in Chinese).

Guan, Q., Zhang, J., Wang, L., Pan, B., Gui, H., Zhang, C., 2013. Discussion of the relationship between dustfall grain size and the desert border, taking the southern border of the Tengger Desert and the southern dust deposit area as an example. Palaeogeography, Palaeoclimatology, Palaeoecology 386, 1–7.

Guo, M., Jie, D., Liu, H., Luo, S., Li, N., 2012. Phytolith analysis of selected wetland plants from Changbai mountain region and implications for palaeoenvironment. Quaternary International 250, 119–128.

Hakanson, L., Jansson, M., 1983. Principles of Lake Sedimentology. Springer-Verlag, Berlin.

Hong, B., Liu, C., Lin, Q., Yasuyuki, S., Leng, X., Wang Y., Zhu, Y., Hong, Y., 2009. Temperature evolution from the $\delta^{18}O$ record of Hani peat, Northeast China, in the last 14000 years. Science in China Series D: Earth Sciences 52(7), 952–964.

Hong, B., Hong, Y., Lin, Q., Shibata, Y., Uchida, M., Zhu, Y., Leng, X., Wang, Y., Cai, C., 2010. Anti-phase oscillation of Asian monsoons during the Younger Dryas period: Evidence from peat cellulose $\delta^{13}C$ of Hani, Northeast China. Palaeogeography, Palaeoclimatology, Palaeoecology 297, 214–222.

Huang, J., Li, A., Wan, S., 2011. Sensitive grain-size records of Holocene East Asian summer monsoon in sediments of northern South China Sea slope. Quaternary Research 75, 734–744.

Huang, T., Cheng, S., Xiao, H., Mao, X., Hu, Z., Zhou, Y., 2015. Early Holocene volcanic eruption discovered in Hani peat bog of NE China and its paleoclimate implication. Quaternary Sciences 35(6), 1500–1508. (in Chinese).

Jie, D., Hu, K., Chen, B., 2010. Dust storms in Northeast China. Geological Publishing House, Beijing.

Johnsen, S.J., Dahl-Jensen, D., Gundestrup, N., Steffensen, J.P., Clausen, H.B. Miller, H., Masson-Delmotte, V., Sveinbjörnsdottir, A.E. White, J., 2001. Oxygen isotope and paleotemperature records from six Greenland ice-core stations: Camp Century, Dye3, GRIP, GISP2, Renland and North GRIP. Journal of Quaternary Science 16(4), 299–307.

Klein, E.S., Yu, Z., Booth, R.K., 2013. Recent increase in peatland carbon accumulation in a thermokarst lake basin in southwestern Alaska. Palaeogeography, Palaeoclimatology, Palaeoecology 392, 186–195.

Lamb, H.H., 1965. The early medieval warm epoch and its sequel. Palaeogeography Palaeoclimatology Palaeoecology 1(65), 13–37.

Lamb, H.H., 1980. Weather and Climate Patterns of the Little Ice Age. Springer Berlin Heidelberg, Berlin.

Lewis,D.W., 1989. Applied Sedimentology. Geological Publishing House, Beijing.

Li, H., Bu, Z., Wang, S., An, Z., Zhao, H., Ma, Y., Chen, X., 2009. Environmental implications of the modern testate amoebae in the peatlands in Changbai Mountains. Quaternary Sciences 29(4), 817–824. (in Chinese).

Li, N., Jie, D., Yang, J., Chen, X., Chen, Y., Hu, C., Qiao, Z., 2014. Grain-size Characteristics and Environmental Significance of Peat Ash in the West Foothill of Changbai Mountain. Acta Sedimentologica Sinica 32(5), 873–883. (in Chinese).

Li, Q., 1991. A primary study on the historical change of Songnen Sandy Land. Chinese Science Bulletin 36, 487–489.

Link, A.G., 1966. Textural classification of sediments. Sedimentology 7(3), 249–254.

Liu, J., 1988. The Cenozoic volcanic episodes in Northeast China. Acta Petrologica Sinica 4(1): 1–10. (in Chinese).

Liu, J., 1989. Vegetational and climatic changes at Gushantun Bog in Jilin, NE China Since 13,000 yr B.P.. Acta Palaeontologica Sinica 28, 495–509. (in Chinese).

Liu, T., 1985. Loess and the Environment. Science Press, Beijing.

Liu, Y., Zhang, S., Liu, J., You, H., Han J., 2008. Vegetation and environment history of Erlongwan Maar Lake during the Late Pleistocene on pollen record. Acta Micropalaeontologica Sinica 25(3), 274–280. (in Chinese).

Liu, Y., Liu, J., Han, J., 2009. Pollen record and climate changing since 12.0 ka B.P. in Erlongwan Maar Lake, Jilin Province. Journal of Jilin University (Earth Science Edition) 39(1), 93–98. (in Chinese).

Lu, H., An Z., 1998. Palaeoclimatic significance of grain size of loess-palaeosol deposit in Chinese Loess Plateau. Science in China (Series D) 41, 626–631.

Ma, C., Zhu, C., Zheng, C., Yin, Q., Zhao, Z., 2009. Climate changes in East China since the late-glacial inferred from high-resolution mountain peat humification records. Science in China Series D: Earth Sciences 52, 118–131.

Makohonienko, M., Kitagawa, H., Naruse, T., Nasu, H., Momohara, A., Okuno, M., Fujiki, T., Liu, X., Yasuda, Y., Yin, H., 2004. Late-Holocene natural and anthropogenic vegetation changes in the Dongbei Pingyuan (Manchurian Plain), northeastern China. Quaternary International 123, 71–88.

Parplies, J., Lücke, A., Vos, H., Mingram, J., Stebich, M., Radtke, U., Han, J., Schleser, G., 2008. Late glacial environment and climate development in northeastern China derived from geochemical and isotopic investigations of the varved sediment record from Lake Sihailongwan (Jilin Province). Journal of Paleolimnology 40, 471–487.

Patterson, E.M., Gillette, D.A., 1977. Commonalities in measured size distribution for aerosols having a soil-derived component. Journal of Geophysical Research 82, 2074–2082.

Pye, K., 1987. Aeolian Dust and Dust Deposits. Academic Press, London.

Qiao, S., 1993. A preliminary study on Hani peat-mire in the west part of the Changbai Mountain. Scientia Geographica Sinica 13, 279–287. (in Chinese).

Qiao, S., Yang, Z., Liu, J., Sun, X., Xiang, R., Shi, X., Fan, D., Saito, Y., 2011. Records of late-Holocene East Asian winter monsoon in the East China Sea: Key grain-size component of quartz versus bulk sediments. Quaternary International 230, 106–114.

Qiu, S., 1989. Study on the formation and evolution of Horqin Sandy Land. Scientia Geographica Sinica 9(4), 317–328. (in Chinese).

Qiu, S., Li, Q., Xia, Y., 1992. Paleosols of sandy lands and environmental changes in the Western Plain of Northeast China during Holocene. Quaternary Sciences 3, 224–232. (in Chinese).

Reimer, P.J., Bard, E., Bayliss, A., Beck, J.W., Blackwell, P.G., Bronk Ramsey, C., Buck, C.E., Edwards, R.L., Friedrich, M., Grootes, P.M., Guilderson, T.P., Haflidason, H., Hajdas, I., Hatté, C., Heaton, T.J., Hoffmann, D.L., Hogg, A.G., Hughen, K.A., Kaiser, K.F., Kromer, B., Manning, S.W., Niu, M., Reimer, R.W., Richards, D.A., Scott, M.E., Southon, J.R., Turney, C.S.M., van der Plicht, J., 2013. IntCal13 and Marine13 radiocarbon age calibration curves 0-50,000 yr cal BP. Radiocarbon 55(4), 1869-1887.

Ren, G., Zhang, L., 1997. Late Holocene vegetation in Maili Region Northeast China, as inferred from a high-resolution pollen record. Acta Botanica Sinica 39(4), 353–362. (in Chinese).

Schettler, G., Liu, J., Mingram, J., Stebich, M., Dulski, P., 2006a. East-Asian monsoon variability between 15,000 and 2000 cal. yr BP recorded in varved sediments of Lake Sihailongwan (northeastern China, LongGang volcanic field). Holocene 16, 1043–1057.

Schettler, G., Liu, Q., Mingram, J., Negendank, J.F.W., 2006b. Palaeovariations in the East-Asian monsoon regime geochemically recorded in varved sediments of Lake Sihailongwan (Northeast China, Jilin province). Part 1: Hydrological conditions and dust flux. Journal of Paleolimnology 35, 239–270.

Schettler, G., Mingram, J., Negendank, J.F.W., Liu, J., 2006c. Palaeovariations in the East-Asian monsoon regime geochemically recorded in varved sediments of Lake Sihailongwan (Northeast China, Jilin province). Part 2: a 200-year record of atmospheric lead-210 flux variations and its palaeoclimatic implications. Journal of Paleolimnology 35, 271–288.

Shao, X., Wang, Y., Cheng, H., Kong, X., Wu, J., Edwards, R.L., 2006. Long-term trend and abrupt events of the Holocene Asian monsoon inferred from a stalagmite $\delta^{18}O$ record from Shennongjia in Central China. Chinese Science Bulletin 51, 221–228.

Smith, L.C., MacDonald, G.M., Velichko, A.A., Beilman, D.W., Borisova, O.K., Frey, K.E., Kremenetski, K.V., Sheng Y., 2004. Siberian Peatlands a Net Carbon Sink and Global Methane Source since the Early Holocene. Science 303, 353–356.

Stebich, M., Mingram, J., Han, J., Liu, J., 2009. Late Pleistocene spread of (cool-) temperate forests in Northeast China and climate changes synchronous with the North Atlantic region. Global and Planetary Change 65, 56–70.

Stebich, M., Rehfeld, K., Schlütz, F., Tarasov P.E., Liu, J., Mingram, J., 2015. Holocene vegetation and climate dynamics of NE China based on the pollen record from Sihailongwan Maar Lake. Quaternary Science Reviews 124, 275–289.

Stuiver, M., Reimer, P.J., 1993. Extended ^{14}C database and revised CALIB radiocarbon calibration program. Radiocarbon 35, 215–230.

Sun, D., An, Z., Su, X., Wu, X., Wang, S., Sun, Q., Rea, D.K., Vandenberche, J., 2001. Mathematical approach to sedimentary component partitioning of polymodal sediments and its applications. Progress in Natural Science 11(5), 374–382.

Sun, Y., Gao, S., Li, J., 2003. Preliminary analysis of grain-size populations with environmentally sensitive terrigenous components in marginal sea setting. Chinese Science Bulletin 48, 184–187.

Visher, G.S., 1969. Grain Size Distributions and Depositional Processes. Journal of Sedimentary Research 39(3), 1074–1106.

Wang, B., Tian, F., Hu, H., 2009. Relationship between fractal dimension of river networks and their climates. Journal of Tsinghua University (Science and Technology) 49(12), 1948–1953. (in Chinese).

Wang, G., Liu, J., Tang, J., 2003. Characteristics and environmental significance of the granularity of swampy sediment in Semi arid Areas. Arid Zone Research 20, 211–216. (in Chinese).

Wang, J., 1989. The gazetteer of Changbai Mountains. Jilin Literature and History Press, Changchun.

Wang, P., Clemens, S., Beaufort, L., Braconnot, P., Ganssen, G., Jian, Z., Kershaw, P., Sarnthein, M., 2005a. Evolution and variability of the Asian monsoon system: state of the art and outstanding issues. Quaternary Science Reviews 24, 595–629.

Wang, Y., Cheng, H., Edwards, R.L., An, Z., Wu, J., Shen, C., Dorale, J.A., 2001. A

High-Resolution Absolute-Dated Late Pleistocene monsoon Record from Hulu Cave, China. Science 294, 2345–2348.

Wang, Y., Cheng, H., Edwards, R.L., He, Y., Kong, X., An, Z., Wu, J., Kelly, M.J., Dykoski, C.A., Li, X., 2005. The Holocene Asian monsoon: Links to Solar Changes and North Atlantic Climate. Science 308, 854-857.

Wang, Y., Cheng, H., Edwards, R.L., Kong, X., Shao, X., Chen, S., Wu, J., Jiang, X., Wang, X., An,Z., 2008. Millennial- and orbital-scale changes in the East Asian monsoon over the past 224,000 years. Nature 451, 1090–1093.

Wentworth, C.K., 1922. A Scale of Grade and Class Terms for Clastic Sediments. Journal of Geology 30(5), 377–392.

Wu, J., Wang, Y., Dong, J., 2011. Changes in East Asian summer monsoon during the Holocene recorded by stalagmite $\delta^{18}O$ records from Liaoning Province. Quaternary Sciences 31(6), 990–998. (in Chinese).

Wu, L., Zhu, C., Li, F., Ma, C., Li L., Meng, H., Liu, H., Wang, X., Tan, Y., Song, Y., 2015. Prehistoric flood events recorded at the Zhongqiao Neolithic Site in the Jianghan Plain, Central China. Acta Geographica Sinica 70(7), 1149–1164. (in Chinese).

Xia, Y., Wang P., 2000. Peat record of climate change since 3000 years in Yangmu, Mishan region. Geographical Research 19, 53–58. (in Chinese).

Xiao, J., Chang, Z., Fan, J., Zhou, L., Zhai, D., Wen, R., Qin, X., 2012. The link between grain-size components and depositional processes in a modern clastic lake. Sedimentology 59, 1050–1062.

Xu, Q., Wang, Z., Xu, Q., Xia, Y., 1994. Pollen analysis of peat marsh in birch forest, the Changbai Mountains and the significance. Scientia Geographica Sinica 14(2), 186–192. (in Chinese).

Xu S., Wang T., 2011. Comparative Study on the Grain Size Characteristics of Loess Deposit both on Miaodao Islands and on the Laizhou Bay plain and its implications for provenance. Procedia Environmental Sciences 10, 1869–1875.

Yuan, B., Deng, C., Lü, J., Jin, C., Wu, Y., 2002. A late Quaternary accumulation period and the prehistoric flood in Beijin Plain. Quaternary Sciences 22(5), 474–482. (in Chinese).

Yang, L., Yue, L., 2013. Horqin Dunefield in Northeastern China in the Last Late Glacial and Holocene as revealed by OSL dating. Quaternary Sciences 33(2), 260–268. (in Chinese).

Yang, Y., Huang, X., Wang, S., Kong, Z., 2001. Study on the mire development and palaeogeographical environment change since the early period of the Holocene in the East Part of the Xiliaohe Plain. Scientia Geographica Sinica 21(3), 242–249. (in Chinese).

Yi, S., Lu, H., Zeng, L., Xu, Z., 2013. Paleoclimate changes and reconstruction of the border of Horqin Dunefield (Northeastern China) since the Last Glacial Maximum. Quaternary Sciences 33(2), 206–307. (in Chinese).

Yu, C., Luo, Y., Sun, X., 2008. A high-resolution pollen records from Ha'ni Lake, Jilin, Northeast China showing climate changes between 13.1 ka cal. BP and 4.5 ka cal. BP. Quaternary Sciences 28(5), 929–938. (in Chinese).

Yu, X., Zhou, W., Liu, X., Zheng, Y., Song, S., 2006. Grain size characteristics of the Holocene peat sediment in eastern Tibetan Plateau and its paleoclimatic significance. Acta Sedimentologica Sinica 12(6), 864–869. (in Chinese).

Yuan, S., Sun, X., 1990. The vegetational and environmental history at the west foot of Changbai

Mountain, Northeast China during the last 10,000 years. Acta Botanica Sinica 32(7), 558–567. (in Chinese).

Zhang, K., Gao, H., Zhang, R., Zhu, Y., Wang Y., 2005. Sources and movement routes of sand-dust aerosols and their impact probabilities on China seas in 2000-2002. Advances in Earth Science 20(6), 627–636.

Zhang, X., Fang, S., Hu, K., Wang, D., 2011. Plaeo-climate analysis of the geochemical element records in the Late Holocene peat deposits of Dunhua Basin, NE China. Arid Land Geography 34(5), 726–732. (in Chinese).

Zhang, X., Hu, K., Wang, D., 2007. Morphological characteristics of phytolith in surface peat deposits of Northeast China. Scientia Geographica Sinica 27, 831–836. (in Chinese).

Zhang, X., Li, Y., Liu, G., Yin, H., 2004. Environmental change in the Northwest Area of Liaoning Province during the middle Holocene. Marine Geology & Quaternary Geology 24(4), 115–120. (in Chinese).

Zhang, Y., Zhu, C., Shi, W., 2002. Middle and Late Holocene climatic changes and sealevel changes and paleo-floods of Maqiao, Shanghai. Marine Sciences 26(1), 54–58. (in Chinese).

Zhang, Z., Xing, W., Lu, X., Wang, G., 2014. The grain-size depositional process in wetlands of the Sanjiang Plain and its links with the East Asian monsoon variations during the Holocene. Quaternary International 349, 245–251.

Zhao, H., Hall, V.A., 2015. Assessing the potential for cryptotephra studies in Northeastern China. The Holocene 25, 772–783.

Zhao, H., Lu, Y., Yin, J., 2005. SAR dating of quartz and geochronology of Holocene sand dune activities in Horqin sandyfield, China. Nuclear Techniques 28(5), 368–374. (in Chinese).

Zhao, L., Satoha, M., Inoue, K., 1997. Clay mineralogy and pedogenesis of volcanic ash soils influenced by tropospheric eolian bust in Changbaishan, Sanjiaolongwan, and Wudalianchi, Northeast China. Soil Science and Plant Nutrition 43(1), 85–98.

Zhao, S., Xia, D., Jin, H., Wen, Y., Liu, J., Liu, B., Li, G., 2013. High-resolution climate evolution record of the Horqin Sandy Land since about 5000 cal. a BP. Quaternary Sciences 33(2), 283–292. (in Chinese).

Zhao, Y., Yu, Z., Zhao, W., 2011. Holocene vegetation and climate histories in the eastern Tibetan Plateau: controls by insolation-driven temperature or monsoon-derived precipitation changes? Quaternary Science Reviews 30, 1173–1184.

Zhao, Y., Yu, Z., Tang, Y., Li, H., Yang,B., Li, F., Zhao, W., Sun, J., Chen, J., Li, Q., Zhou, A., 2014. Peatland initiation and carbon accumulation in China over the last 50,000 years. Earth-Science Reviews 128, 139–146.

Zhou, X., Yang, W., Xiang, R., Wang, Y., Sun, L., 2014. Re-examining the potential of using sensitive grain size of coastal muddy sediments as proxy of winter monsoon strength. Quaternary International 333, 173–178.

Zhou, W., Zheng, Y., Meyers, P.A., Jull, A.J.T., Xie, S., 2010. Postglacial climate-change record in biomarker lipid compositions of the Hani peat sequence, Northeastern China. Earth & Planetary Science Letters 294, 37–46.

Zhu, C., Yu, S., Lu, C., 1997. The study of Holocene Environmental Archaeology and extreme flood disaster in the three gorges of the Changjiang River and the Jianghan Plain. Acta Geographica Sinica 52(3), 269–278. (in Chinese).

Zhu, K., 1973. Preliminary study on climate change over last 5000 years in China. Science in

China (2), 168–189. (in Chinese).

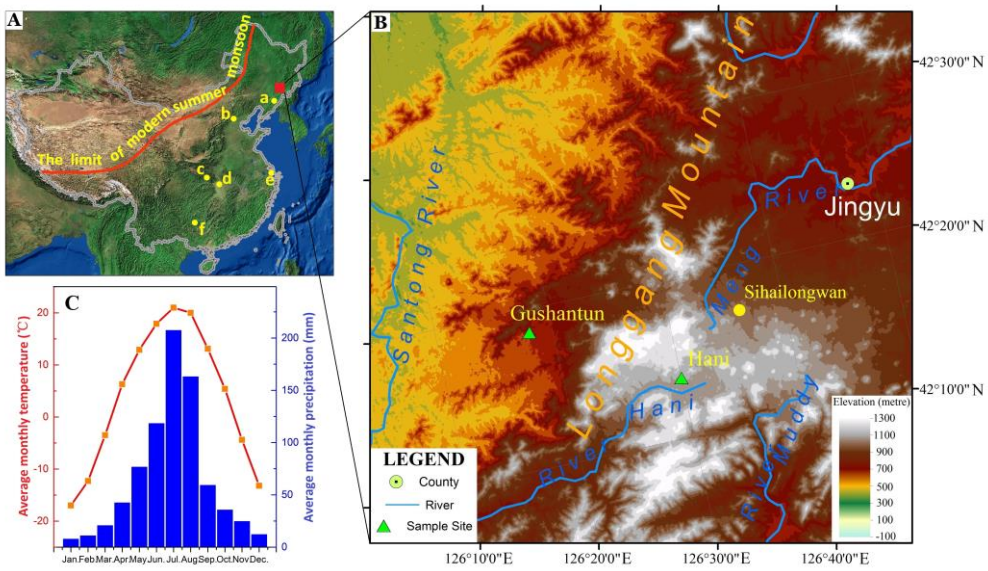

Fig. 1. (A) Location of the study region, key records discussed in the text and shown in Figs. 8 and 9, respectively: (a) Nuanhe Cave; (b) paleo-flood records in Beijing Plain; (c) Shanbao Cave; (d) Zhongqiao archaeological site; (e) Maqiao archaeological site; (f) Dongge Cave, the limit of the modern summer monsoon was modified after Gao, 1962. (B) Location and geographical setting of Hani and Gushantun peatlands, Lake Sihailongwan. (C) Climatic pattern in the study area. Diagrams show average monthly temperature and precipitation of Jingyu station from 1981 to 2010.

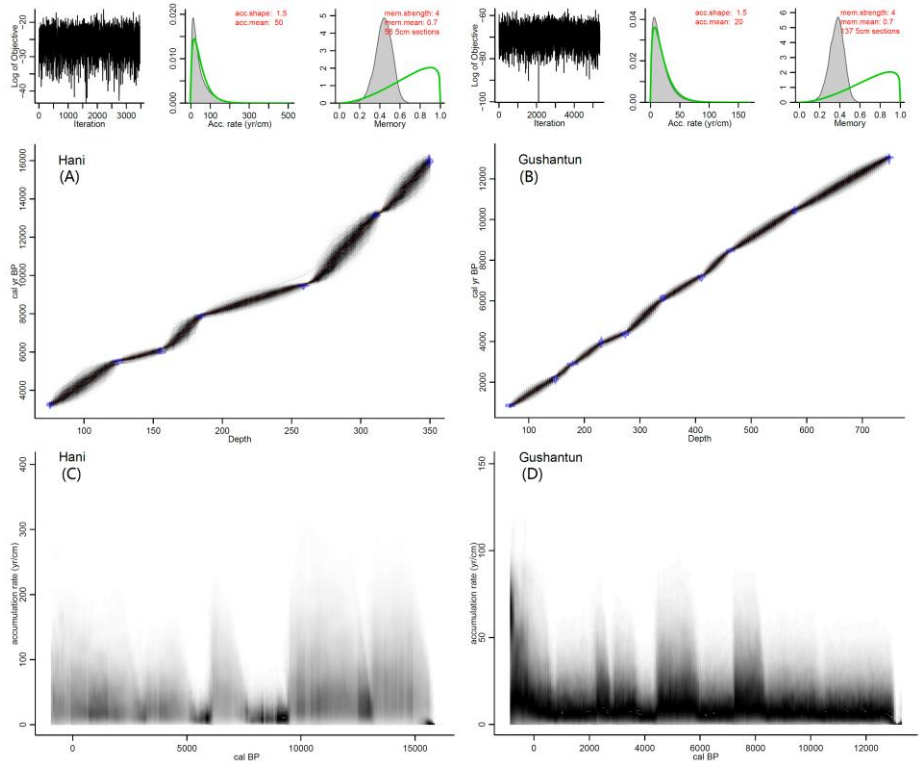

Fig. 2. ‘Bacon’ age-depth models and accumulation rate plots for Hani(A, C) and Gushantun (B, D) cores. The best estimates for calibrated age are shown in red. The upper and lower estimates are shown in gray.

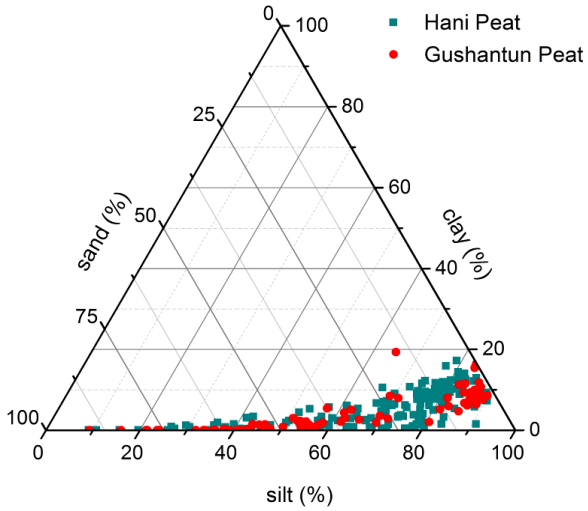

Fig. 3. Textural composition of peat sediments in the Changbai Mountains.

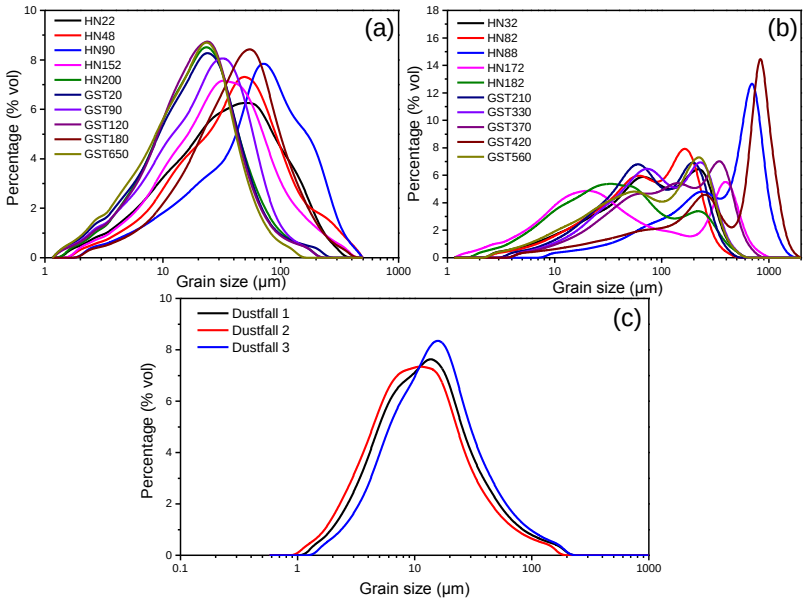

Fig. 4. Representative grain size frequency distribution curves of (a) peat samples showing unimodal distribution, (b) peat samples showing multimodal distribution, and (c) dustfall samples. Sample numbers represent depth (cm) in the Hani (HN) and Gushantun (GST) peat cores.

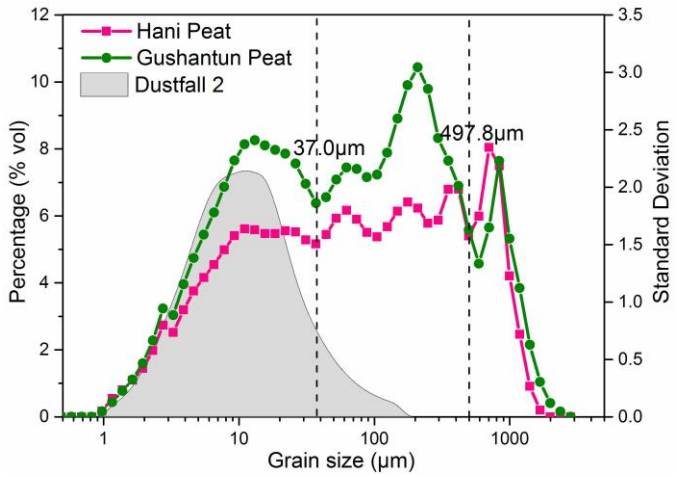

Fig. 5. Grain-size classes *vs.* standard deviation diagram of Hani and Gushantun peat cores. Gray area shows the grain size distribution of dustfall sample.

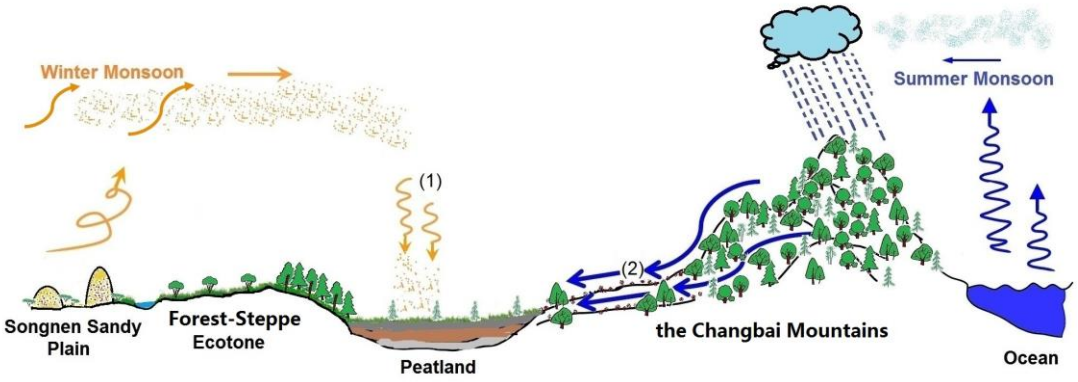

Fig. 6. Schematic diagram indicating the sources and deposition process of the grain size components in peatland sections in the Changbai Mountains. (1) and (2) denote processes of particle transportation described in the text.

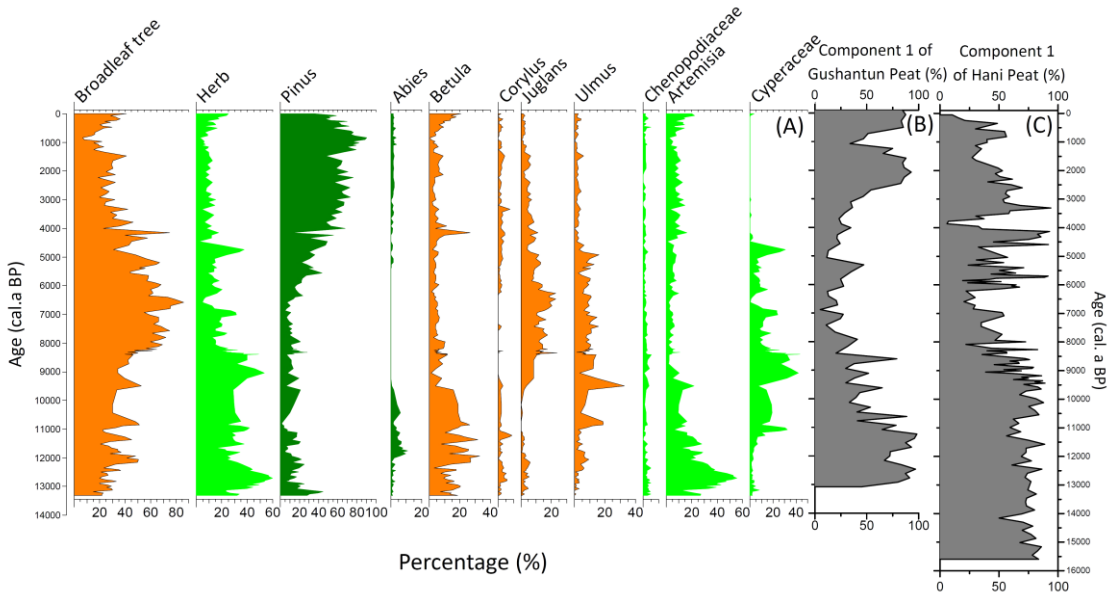

Fig. 7. Comparisons of the component 1 content in Hani (C) and Gushantun (B) peat cores with simplified pollen diagram (Cui et al., 2006; Yu et al., 2008) of Hani peat (A).

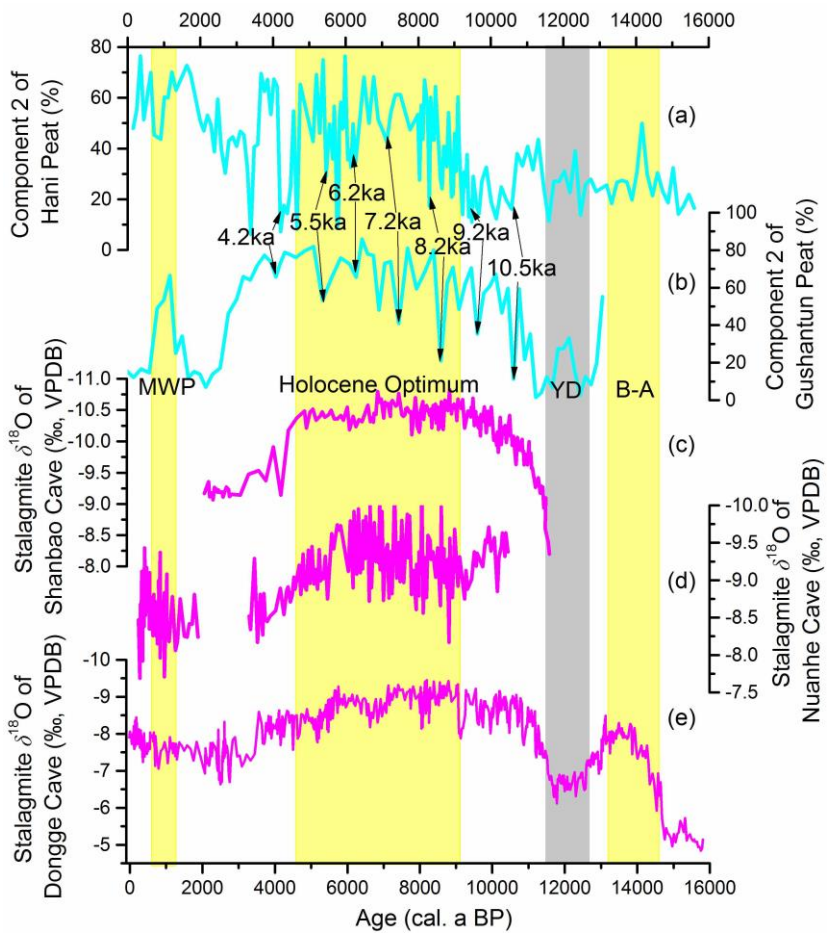

Fig. 8. Comparisons of the grain size record of peat sediments from Changbai Mountains with several absolutely dated East Asian Monsoon records in China.
(a) percentage of Component 2 in core Hani (This study); (b) percentage of Component 2 in core Gushantun (This study); (c) $\delta^{18}O$ record of stalagmite SB10 from Shennongjia, Central China (Shao et al., 2006); (d) stalagmite $\delta^{18}O$ record from Nuanhe cave, NE China (Wu et al., 2011); (e) stalagmite $\delta^{18}O$ record from Dongge cave, SW China (Dykoski et al., 2005). MWP denotes Medieval Warm Period. YD denotes Younger Dryas. B-A denotes Bølling-Allerød interstadial.

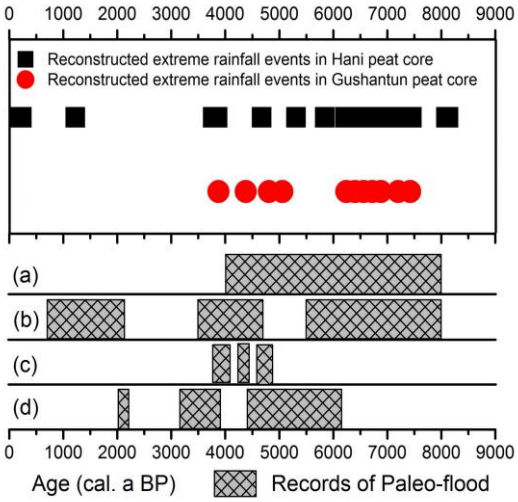

Fig. 9. The comparison between reconstructed extreme rainfall events based on grain size Component 3 in peat cores from Changbai Mountains (This study) and previous published paleo-flood records in China.
(a) paleofloods in Beijing Plain (Yuan et al., 2002); (b) paleoflood records inferred from archaeological sites in the Three Gorges area and the Jianghan Plain (Zhu et al., 1997); (c) paleoflood records inferred from Zhongqiao archaeological sites of the Jianghan Plain (Wu et al., 2015); (d) paleoflood records inferred from Maqiao archaeological sites, Eastern China (Zhang et al., 2002).

Table 1 AMS radiocarbon dates of samples from Hani and Gushantun peat profiles

Sample Location	Depth (cm)	Lab. Code*	Material	AMS ^{14}C BP	Uncertainty	2σ-range cal. BP	Median age, cal. BP
Hani	75-76	BA091607	Bulk organic matter	3040	35	3157-3358	3246
Hani	124-125	BA091608	Bulk organic matter	4785	35	5335-5596	5518
Hani	184-185	BA091610	Bulk organic matter	7045	40	7794-7954	7885
Hani	258-259	BA091613	Bulk organic matter	8435	40	9330-9530	9470
Hani	310-311	BA091614	Bulk organic matter	11285	45	13062-13242	13136
Hani	349-350	BA091615	Mud	13280	50	15767-16156	15968
Gushantun	66-67	BA10856	Bulk organic matter	935	25	793-919	853
Gushantun	147-148	BA10858	Bulk organic matter	2140	45	1998-2306	2130
Gushantun	178-179	BA10859	Bulk organic matter	2795	25	2803-2961	2898
Gushantun	230-231	BA10860	Bulk organic matter	3645	50	3839-4319	3966
Gushantun	273-274	BA10861	Bulk organic matter	3930	30	4249-4499	4366
Gushantun	361-362	BA10863	Bulk organic matter	5375	45	6005-6282	6184
Gushantun	410-411	BA10864	Bulk organic matter	6250	40	7020-7264	7192
Gushantun	462-463	BA10865	Bulk organic matter	7685	40	8404-8548	8474
Gushantun	578-579	BA10867	Bulk organic matter	9270	40	10296-10569	10454
Gushantun	748-749	BA10871	Mud	11165	50	12883-13132	13041

* Peking University Accelerator Mass Spectrometry Laboratory, China.

Table 2 Grain-size classes *vs.* standard deviation values of Hani and Gushantun peat cores

Grain size (μm)	S.D.$_{HN}$	S.D.$_{GST}$	Grain size (μm)	S.D.$_{HN}$	S.D.$_{GST}$
2816.0	0.00	0.00	37.0	1.51	1.86
2368.0	0.00	0.05	31.1	1.54	2.03
1991.0	0.00	0.12	26.2	1.61	2.21
1674.0	0.06	0.30	22.0	1.62	2.29
1408.0	0.27	0.63	18.5	1.60	2.33
1184.0	0.72	1.12	15.6	1.60	2.36
995.6	1.23	1.55	13.1	1.63	2.41
837.2	2.19	2.23	11.0	1.64	2.37
704.0	2.35	1.65	9.3	1.58	2.23
592.0	1.75	1.33	7.8	1.46	2.00
497.8	1.58	1.63	6.5	1.33	1.78
418.6	1.98	2.01	5.5	1.21	1.59
352.0	1.98	2.23	4.6	1.10	1.38
296.0	1.71	2.43	3.9	0.93	1.16
248.9	1.69	2.86	3.3	0.73	0.89
209.3	1.82	3.04	2.8	0.80	0.94
176.0	1.87	2.89	2.3	0.58	0.67
148.0	1.79	2.60	2.0	0.42	0.47
124.5	1.66	2.30	1.6	0.32	0.33
104.7	1.57	2.11	1.4	0.24	0.23
88.0	1.61	2.09	1.2	0.16	0.13
74.0	1.72	2.16	1.0	0.05	0.05
62.2	1.80	2.17	0.8	0.00	0.00
52.3	1.73	2.07	0.7	0.00	0.00
44.0	1.59	1.91	0.6	0.00	0.00